Macromolecules 1992, *25*, 3284-32

Electrically Conductive Semiinterpenetrating Polymer Networks of Poly(3-octylthiophene)

Yading Wang and M. F. Rubner*

Department of Materials Science and Engineering, Massachusetts Institute of Technology, Cambridge, Massachusetts 02139

Received August 28, 1991

ABSTRACT: Electrically conducting, semiinterpenetrating polymer networks (semi-IPNs) were synthesized from soluble poly(3-octylthiophene), styrene monomer, and a cross-linking agent. By controlling the level of cross-linking of the polystyrene component, it was possible to create semi-IPNs with highly dispersed microdomains of the conjugated polymer. For example, semi-IPN samples containing 20% poly(3-octylthiophene) (P3OT) and 10% divinylbenzene (DVB) exhibited very finely dispersed P3OT domains on the order of 1000 Å. This particular cross-linking level also produced semi-IPNs with a very low percolation threshold (ca. 3 vol % P3OT). The conductivity stability of $FeCl_3$-doped samples containing 20% P3OT and cross-linked with 10% DVB was found to be considerably enhanced, thereby supporting the hypothesis that improved stability in these materials may be achieved by restricting their chain mobility.

1. Introduction

For some time now it has been recognized that the properties of electrically conductive polymers can be substantially altered and in many cases significantly improved by blending with suitable insulating host polymers. Most notably, this approach has been quite successful at producing electrically conductive blends with a wide range of interesting mechanical and electrical properties. The techniques utilized to date include chemical[1-4] and electrochemical[5-16] in situ polymerization, melt and solution processing,[17-25] sintering,[26] and precursor manipulation.[27-31] In all cases, however, blending has had very little impact on the environmental stability of the conducting polymer. One of the major limitations of the blending approach is that it almost always produces a highly heterogeneous two-phase system. This high level of phase separation is a direct consequence of the small entropy of mixing generally associated with macromolecular systems. As a result of this, it is very difficult to achieve the level of molecular intermixing needed to significantly alter the physical properties of each of the components of the blend.

We have recently reported that the chain mobility of the doped poly(3-alkylthiophenes) dramatically influences the stability of the electrical conductivity of these materials.[32] In essence, the lower the chain flexibility, the more stable is the polymer. It was therefore proposed that the conductivity stability might be improved by restricting the chain mobility of these conducting polymers. As indicated above, this cannot be readily accomplished by simple blending techniques as the resultant two-phase morphology is not sufficiently intermixed to restrict the chain mobility of the conducting polymer. It is possible to achieve this goal, however, through the use of semiinterpenetrating polymer networks. Semiinterpenetrating polymer networks are typically two-component systems in which one of the polymers has been cross-linked into a covalently linked network.[33] Since the formation of the network is accomplished in the presence of the second polymer, the level of phase mixing is usually significantly higher than that obtained by blending. In addition, by controlling the synthesis process and the level of cross-linking, it is possible to vary the morphology of the semi-IPN over a very wide range. Thus, in sharp contrast to blending, one now has the ability to manipulate the level of molecular dispersion of the two components, the size of their domains, and the nature of their interfacial regions. Previous studies have indicated that the cross-linked polymer in a semiinterpenetrating polymer network can be used to reduce the molecular mobility of the non-cross-linked polymer.[34] Thus, this approach seems well suited to improving the conductivity stability of the poly(3-alkylthiophenes).

In this paper, we describe the synthesis, molecular organization, and conductivity stability of semi-IPNs comprised of cross-linked polystyrene and poly(3-octylthiophene). Although a large number of studies have been conducted on various conducting polymer composites and blends, we believe that this represents the first investigation of an electrically conductive semiinterpenetrating polymer network.

2. Experimental Section

2.1. Synthesis of Poly(3-octylthiophene). The starting monomer, 3-octylthiophene (3OT), was synthesized via the coupling of octylmagnesium bromide with 3-bromothiophene in the presence of $Ni(dppp)Cl_2$ according to the method of Kumada et al.[35] The monomer was purified prior to use by distillation under reduced pressure. Polymerization of 3OT was achieved following the $FeCl_3$ method of Sugimoto et al.[36] Special precautions were taken to avoid oxygen and moisture during the polymerization. The as-prepared polymer was extracted in a Soxhlet extractor consecutively with methanol and acetone for 2 weeks. The purified polymer was then dissolved in warm chloroform, filtered, and cast into free-standing films under a flow of nitrogen. Molecular weight characterization of the polymer was performed on a Waters Associates 6000A gel permeation chromatograph using THF as the carrier solvent and polystyrene standards for calibration. The weight-average molecular weight (polystyrene equivalents) was found to be 64 900, and the number-average molecular weight was 8230.

2.2. Synthesis of the Semiinterpenetrating Polymer Networks. The purified P3OT was dissolved in solutions of styrene and divinylbenzene (DVB; dried over molecular sieves) to give mixtures with different P3OT volume fractions (3, 5, 10, 15, 20, and 25%) and different DVB mole fractions (relative to the number of moles of styrene) (0, 1, 2, 5, 10, 16, and 23% for the 20% P3OT samples; 10% for the rest). To the mixtures was also added 1% (by weight) AIBN as the initiator. Three freeze-thaw cycles were performed after the solutions became homogeneous to avoid the presence of oxygen in the reaction flasks. The reaction flasks were slowly rotated in a horizontal position in order to coat the inner flask walls with uniform thin films of the reaction mixtures. The rotating flasks were then placed in an oven at 90 °C. After 2-3 h the temperature was raised to 110

0024-9297/92/2225-3284$03.00/0

°C for an additional 1-2 h to allow complete reaction. The reaction flasks were then allowed to cool to room temperature, and the semi-IPN films were removed from the flask walls using an ultrasonic treatment. The free-standing films were then dried under vacuum at 60 °C for 24 h. The thickness of the films ranged from 40 to 90 μm. Doping of the semi-IPN free-standing films was accomplished using ferric chloride solutions: 30 g/L of $FeCl_3$ dissolved in a mixture of nitromethane and benzene (volume ratio 2/1). Benzene was used as a cosolvent to swell the semi-IPNs and thereby facilitate penetration of the dopant into the networks.

2.3. Stability Tests. The stability tests were carried out in an environment-controllable glass chamber whose temperature was regulated using suitable circulating baths. Dry nitrogen was created by passing the prepurified gas consecutively through a concentrated sulfonic acid column and a calcium oxide column. Laboratory air was air-conditioned and had a relative humidity of about 30% at room temperature (22 °C). All of the environmental tests were carried out under static conditions rather than with a flowing stream of the gas. A four-lead method was used to measure the conductivity, and an Electrodag 502 was used to make electrical contact with the films. Constant currents were generated from a Keithley 224 programmable current source, and the voltages were recorded on strip-chart recorders.

2.4. Characterization of the Semi-IPNs. UV-vis spectra of thin semi-IPN films were recorded on an Oriel 77200 250-mm spectrometer in a laboratory atmosphere at room temperature. DSC studies of the samples were conducted on a Perkin-Elmer DSC7 differential scanning calorimeter under nitrogen at a scanning rate of 10 °C/min. Bright-field optical micrographs of the semi-IPN films were taken in the transmission mode with a Nikon HFX-II microscope. Scanning transmission electron microscopy (STEM) of cryomicrotomed samples (20% P3OT/10% DVB) was performed on a Vacuum Generators VG HB5 scanning transmission electron microscope.

3. Results and Discussion

The morphological features of semi-IPNs, such as their level of phase mixing, the molecular and supermolecular organizations of their domains, and the nature and form of their interfacial zones, are known to be strongly influenced by the amount of cross-linking introduced during network formation. These features, in turn, determine the macroscopic properties exhibited by the semi-IPN. In order to examine the effects that different cross-linking levels have on the conductivity and conductivity stability of the P3OT-based semi-IPNs, samples were prepared with different DVB mole percentages ranging from 0 to 23% (based on the amount of styrene monomer present). The influence of the level of cross-linking was examined with films containing 20% P3OT since this conjugated polymer amount produced films with good film quality and high electrical conductivities after doping. According to Sperling's nomenclature,[33] these semi-IPNs are of the second kind; i.e., they consist of a non-cross-linked polymer (polymer I; P3OT) and a cross-linked polymer (polymer II; polystyrene). As-prepared films containing 5, 10, 16, and 23% DVB appeared completely uniform to the eye, whereas films prepared with no DVB or with only 1 or 2% DVB appeared highly heterogeneous. This immediately suggests that the level of cross-linking does indeed strongly influence the morphology of the semi-IPN. The conductivity of samples doped with $FeCl_3$ was in the range of 0.01–0.1 S/cm, which is 1–2 orders of magnitude lower than that of free-standing films of doped P3OT. Essentially all of the P3OT in the semi-IPNs could be extracted by solvents (chloroform, THF, etc.) provided that sufficient time was allowed for the extraction process.

3.1. Spectroscopic Studies. Parts a and b of Figure 1 display the UV-vis spectra of the semi-IPNs fabricated with different levels of cross-linking. Also included in Figure 1a is the spectrum of the semi-IPN liquid mixture (20% P3OT) before polymerization of the styrene/DVB monomer system (curve b) and a spectrum of a thin film of neutral P3OT (curve a). The primary absorption band present in all of these curves is the well-known $\pi-\pi^*$ interband transition of the conjugated polythiophene backbone (λ_{max} at about 470 nm for the cast film of pure P3OT). After dissolution of the P3OT in the liquid styrene/DVB mixture, it can be seen that the absorption band of the conjugated polymer becomes narrower and loses its lower energy tail (curve b). The elimination of the longer wavelength portion of this absorption band indicates that the dissolved polymer chains have assumed a shorter average conjugation length due to dissolution in the monomeric solvent. In other words, the π-electrons of the conjugated backbone have become more localized due to the conformational disorder introduced when the polymer is dissolved. The narrowing of the absorption band reflects the fact that many of the different environments available to the conjugated chains (such as crystalline and paracrystalline environments) have been disrupted upon solvation, thereby leaving a much narrower distribution of shorter effective conjugation lengths.

Spectra c–h were recorded after the polymerization of the semi-IPN solutions. The P3OT content was 20% for samples c–g and 5% for sample h. In all cases, there is a reestablishment of the lower energy absorption present in the film of pure P3OT. Specifically, it is now possible to identify at least three major peaks in each of these spectra: a low-energy peak at about 605 nm which arises due to conjugated chains present in well-defined, highly ordered domains, a higher energy peak at about 500 nm which is characteristic of conjugated chains present in less ordered, perhaps more dispersed domains, and a peak at about 460 nm which is due to conjugated chains present in highly disordered regions of the film such as in the interfacial zones. The emergence of the lower energy peaks in these spectra indicates that the conjugated polythiophene chains now exist in a variety of molecular environments which impose different constraints on the planarity of their backbones. In particular, the development of an intense low-energy shoulder suggests that many of the polythiophene chains have aggregated into well-ordered crystalline or paracrystalline domains. Thus, a significant amount of phase separation occurs during the formation of the glassy polystyrene network. It can be seen, however, that the lowest energy peak is most pronounced in the film formed without any cross-linking but becomes significantly less intense in the cross-linked films. Thus, the ability of the conjugated chains to phase separate into well-ordered domains is clearly inhibited by the formation of the polystyrene network. It is interesting to note that the smallest low-energy shoulder is found in sample h which has only 5% P3OT. This implies that crystallization of the polythiophene chains is further restricted in semi-IPNs with lower P3OT contents. The presence of a stronger low-energy absorption in the semi-IPNs as compared to the thin film of pristine P3OT simply reflects the fact that the semi-IPNs were annealed during network formation which clearly promotes the development of a greater fraction of ordered polythiophene chains.

3.2. Thermal Analysis. The DSC thermograms of the semi-IPN samples with different levels of cross-linking are displayed in Figure 2. The heat flow scale is arbitrary in this case since the curves have been normalized for the sake of clarity. Curve g represents the DSC thermogram of pure P3OT whereas curve h is that of a polystyrene sample cross-linked with 10% DVB. The DSC thermogram of P3OT exhibits a melting transition at about 62

Macromolecules, Vol. 25, No. 12, 1992

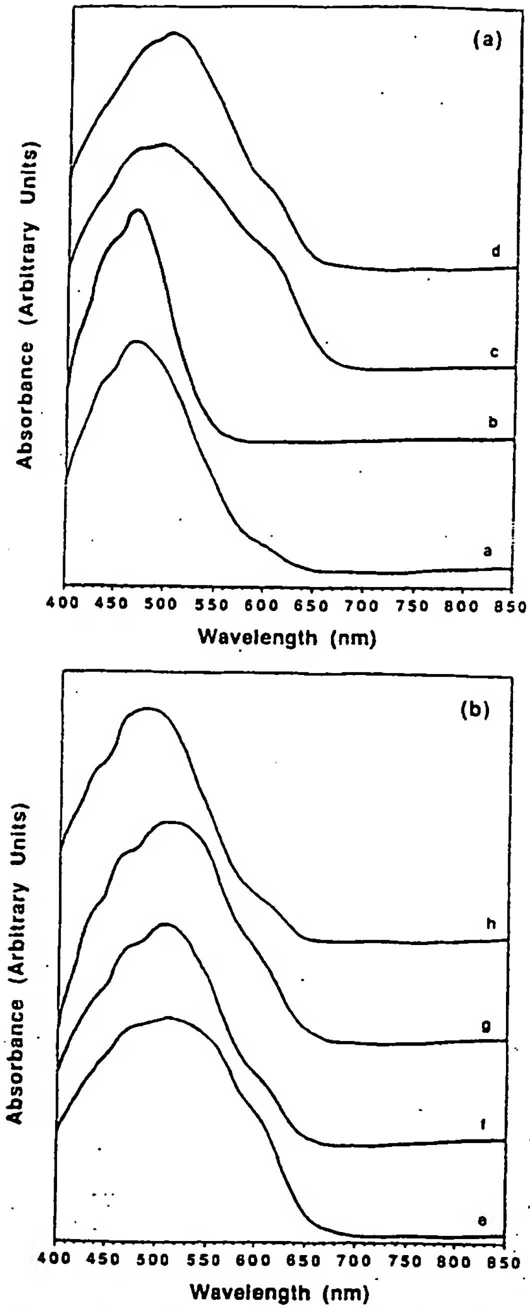

Figure 1. (a) UV–vis spectra of the semi-IPNs and related materials. a: Neutral P3OT. b: P3OT (20%) solution in styrene and DVB. c: Semi-IPN (20% P3OT)/0% DVB. d: Semi-IPN (20% P3OT)/2% DVB. (b) UV–vis spectra of the semi-IPNs and related materials. e: Semi-IPN (20% P3OT)/5% DVB. f: Semi-IPN (20% P3OT)/10% DVB. g: Semi-IPN (20% P3OT)/16% DVB. h: Semi-IPN (5% P3OT)/10% DVB.

°C but no indication of a glass transition temperature within the experimental temperature range. We attribute the melting peak, which can also be found in the DSC thermograms of samples a–f, to a thermally induced disordering of the octyl side chains of P3OT. These peaks did not show up (or were extremely weak) in the thermograms of samples evaluated immediately after synthesis. Only after storage of the samples at room temperature for at least a week did the melting transitions become conspicuous. Thus, the development of this form of ordering within the P3OT regions appears to be a very slow process. Note that the melting peak occurs at about 62 °C for all of the samples with the exception of sample e (semi-IPN/10% DVB) which exhibits a melting transition at about 50 °C. The melting point depression of this sample suggests that this particular semi-IPN composition produces a higher level of phase mixing. The consequences of this higher level of phase mixing will become apparent shortly.

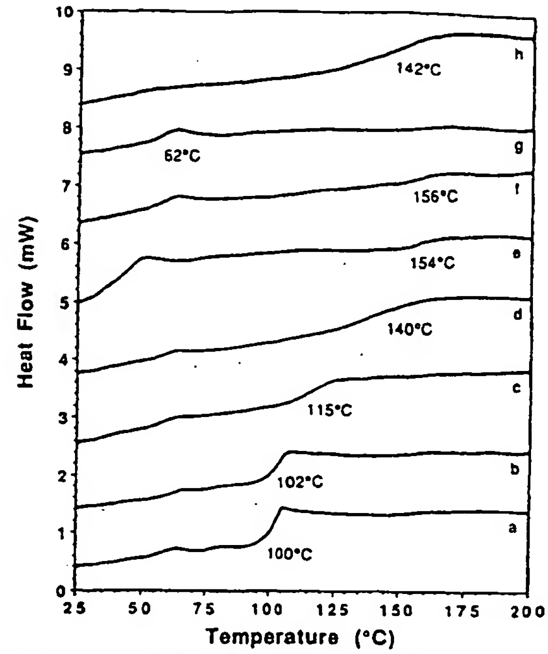

Figure 2. DSC thermograms of the semi-IPNs and related materials: (a) semi-IPN (20% P3OT)/0% DVB, (b) semi-IPN (20% P3OT)/1% DVB, (c) semi-IPN (20% P3OT)/2% DVB, (d) semi-IPN (20% P3OT)/5% DVB, (e) semi-IPN (20% P3OT)/10% DVB, (f) semi-IPN (20% P3OT)/16% DVB, (g) neutral P3OT, (h) polystyrene/10% DVB.

The glass transition temperatures observed in these thermograms are due to the polystyrene component of the semi-IPN. For the sample prepared without any cross-linking (sample a 0% DVB), this transition occurs at the same temperature of pure polystyrene, about 100 °C. As expected, as the level of cross-linking in the semi-IPN increases, the glass transition temperature is also seen to increase (from 100 to about 156 °C). It is interesting to note, however, that the glass transition temperature of the semi-IPN cross-linked with 10% DVB (curve e) is over 10 °C higher than that observed in a pure sample of polystyrene cross-linked with 10% DVB (curve h). This suggests that the ability of the cross-linked network to inhibit the chain mobility of the polystyrene phase is enhanced in the semi-IPN. This may be due to the creation of more effective cross-links or a higher degree of molecular interpenetration with the P3OT phase.

3.3. Thermal Stability of the Electrical Conductivity. Figures 3 and 4 display the conductivity (normalized to the value at t = 0 min) of various $FeCl_3$-doped semi-IPNs (containing 20% P3OT) and related materials recorded at different temperatures (80 °C for Figure 3 and 120 °C for Figure 4) as a function of time. A quick survey of the data collected at 80 °C reveals that

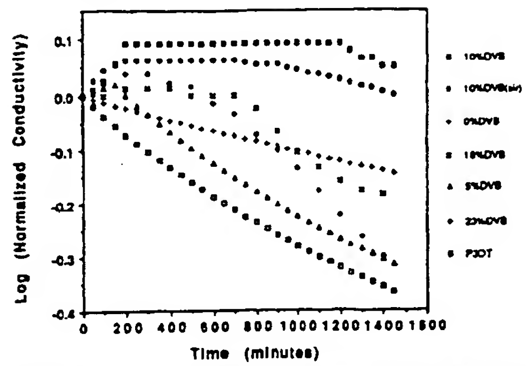

Figure 3. Conductivity stability of the semi-IPNs (20% P3OT) and related materials at 80 °C under dry nitrogen (or in laboratory air as indicated).

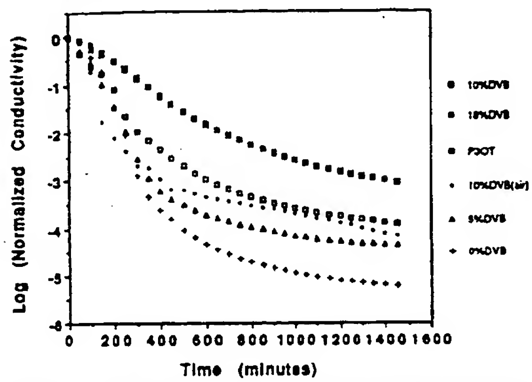

Figure 4. Conductivity stability of the semi-IPNs (20% P3OT) and related materials at 120 °C under dry nitrogen (or in laboratory air as indicated).

all of the semi-IPNs exhibit a better conductivity stability than P3OT. Most notably, the samples prepared with 10% DVB are significantly more stable than samples prepared from the pure conjugated polymer or any of the various network compositions. It can also be seen that all of the semi-IPN samples exhibit increases in conductivity during the first few hundred minutes of the stability tests (this effect is most pronounced in the 10% DVB samples). Since the data were recorded after the samples were equilibrated at the test temperature, this phenomenon cannot be attributed to a sample thermally activated conduction process. This thermally induced conductivity increase is therefore believed to be due to an additional doping process that occurs at elevated temperatures. Similar behavior has also been observed in the $FeCl_3$-doped P3ATs[32] although to a much lesser extent. The fact that the additional doping process is more pronounced in the semi-IPNs suggests a number of interesting possibilities. The first possibility may simply reflect the fact that a larger amount of unreacted $FeCl_3$ or its doping byproducts remain trapped in the network after doping. This hypothesis, however, does not explain the fact that the highest level of additional doping is observed in samples cross-linked with 10% DVB and not the more highly cross-linked samples. In addition, a more highly cross-linked sample would also be less likely to absorb a large excess of the dopant. The second possibility is that the samples prepared with 10% DVB are significantly more stable than samples prepared with a lesser or greater amount of the cross-linking agent. Clearly, the thermally activated additional doping process competes directly with the normal conductivity degradation process. An intrinsically more stable material would therefore be able to benefit more from this process than a less stable material. All of these results indicate that the morphology of the 10% DVB composition is particularly well suited for enhancing the stability of its conducting polymer component. The reason for the significantly better conductivity stability of this composition will become apparent shortly.

The conductivity of the semi-IPN/10% DVB sample increases 23% in the first 200 min at 80 °C due to the thermally activated additional doping process and then remains level for another 1000 min before starting to decay at 1200 min. An extended stability test at 80 °C on this sample revealed that the time for its conductivity to drop by 1 order of magnitude ($t_{1/10}$) at this temperature is about 16 000 min. In contrast, the $t_{1/10}$ value for pure P3OT is about 1900 min. Even under a laboratory-air atmosphere, the $FeCl_3$-doped semi-IPN/10% DVB composition is still much more stable than doped P3OT in nitrogen. Also note that the sample prepared without any cross-linking of the polystyrene phase is not as stable as the 10% DVB material. This rules out the possibility that the significantly improved stability of the 10% DVB semi-IPN simply reflects the better barrier properties of the glassy polystyrene matrix. In addition, the barrier properties of the polystyrene matrix, whether cross-linked or not, should not have a bearing on the samples evaluated in a dry-nitrogen atmosphere. As can be seen in Figure 3, the conductivity stability of the 10% DVB sample is diminished when it is exposed to humid air. This indicates that ambient species do get through the barriers in the network and accelerate the degradation of the conductivity.

At 120 °C under dry nitrogen (see Figure 4) the improvement in stability is not as significant. In fact, the samples with 0% and 5% DVB are now less stable than the pure P3OT. In the case of the 0% DVB sample, this temperature is greater than the glass transition temperature of the polystyrene matrix. The added molecular mobility of the polystyrene matrix must therefore better facilitate disorder-inducing conformational transitions of the P3OT chains. The increased conformational activity of the P3OT chains would, in turn, assist in the thermal dedoping process which is known to be strongly enhanced by increased chain mobility.[32] Since the onset of the glass transition temperature of the 5% DVB sample is near 120 °C, a similar argument could be used to explain its lower stability. There are only two semi-IPNs (10% DVB and 16% DVB) that are more stable than P3OT at this temperature. The time for the conductivity to decay by 1 order of magnitude at 120 °C is about 330 min for these two samples as compared to about 180 min for the P3OT. Interestingly, these two conductivity–time curves are identical, as shown in Figure 4. The onset temperatures of the glass transition of these two samples are much higher than 120 °C, thereby insuring less conformation activity and a better conductivity stability. The fact that the two stability curves overlap with each other suggests that very similar environments exist for the P3OT chains in the semi-IPNs at 120 °C. Thus, the morphological differences between these samples at 80 °C are essentially eliminated at 120 °C. The greater stability in this case is still best attributed to the mobility-restricting effect of the semi-IPN network rather than the barrier properties of the cross-linked polystyrene matrix. Indeed, when the doped semi-IPN/10% DVB sample was exposed to humid air at 120 °C, the decrease in the conductivity stability (represented by dots in Figure 4) is significant, indicating that

 Macromolecules, Vol. 25, No. 12, 1992

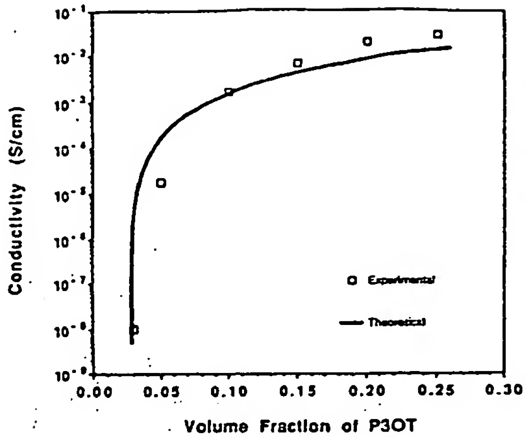

Figure 5. Electrical conduction threshold of the semi-IPN/10% DVB samples. Open squares represent the experimental data and the solid curve is theoretical.

the barrier properties of the sample at this temperature are very poor.

3.4. Electrical Conduction Threshold. The manipulation of conducting polymers via the fabrication of semi-IPNs provides a unique opportunity to control the morphological features of electroactive multicomponent systems. Of particular interest is the development of a two-component system in which microdomains of the conducting phase are molecularly dispersed in an insulating matrix. Such molecular composites are expected to exhibit very low percolation thresholds and hence high electrical conductivities with low loadings of the conducting phase. In order to determine the percolation threshold of the P3OT-based semi-IPNs, the conductivity of a series of samples containing different volume fractions of P3OT and a fixed DVB level of 10% were examined. Figure 5 displays the conductivity–composition plot of the $FeCl_3$-doped semi-IPNs with different volume fractions of P3OT. A sharp transition in the composition dependence of the conductivity takes place between 3 and 5% P3OT, indicating that the percolation threshold for electrical conduction in this system is very low.

According to percolation theory[37] and previous studies on conducting polymer systems,[38,39] a scaling law (eqs 1 and 2), is applicable to the conductivities of multiphase systems.

$$\sigma = C(f - f_c)^t \tag{1}$$

$$\log \sigma = \log C + t \log (f - f_c) \tag{2}$$

In these equations, f represents the volume fraction of the conducting component, f_c is the critical volume fraction (percolation threshold), t is a universal exponent, and C is an arbitrary constant. By fitting the experimental data to a plot of $\log \sigma$ vs $\log (f - f_c)$, it is therefore possible to estimate the percolation threshold. In this case, such a fit reveals a percolation threshold of about 2.8% P3OT and an exponent value of 3.2. This percolation threshold is surprisingly low as compared to most conducting polymer composites or blends.[13,25,27] Note also that even at 5% P3OT, the doped semi-IPN is already in the semiconducting range. This is very interesting because the compromise in mechanical properties of a host polymer will generally be insignificant if only a few percent of the conducting component is incorporated into the matrix.

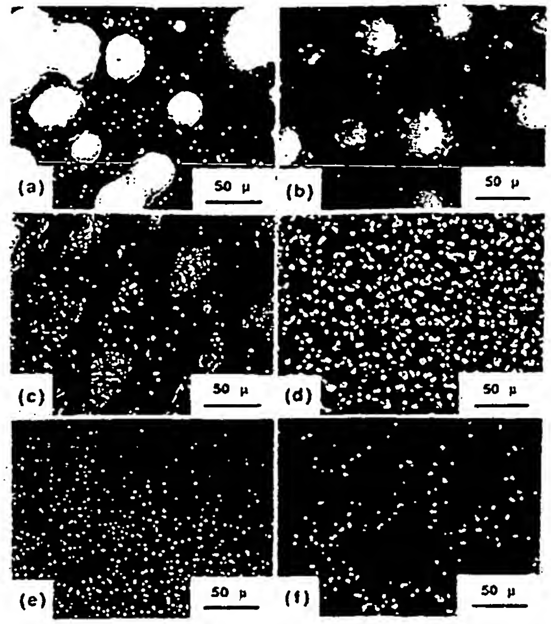

Figure 6. Optical micrographs of the semi-IPNs and related materials: (a) semi-IPN (20% P3OT)/0% DVB, (b) semi-IPN (20% P3OT)/1% DVB, (c) semi-IPN (20% P3OT)/2% DVB, (d) semi-IPN (20% P3OT)/5% DVB, (e) semi-IPN (20% P3OT)/10% DVB, (f) semi-IPN (20% P3OT)/16% DVB.

The theoretically predicted percolation threshold expected for a composite consisting of conductive hard-core spheres dispersed within an insulating matrix is 0.164 ± 0.020.[40,41] In fact, a percolation threshold of 16% has been observed in solution-processed composites fabricated from poly(3-hexylthiophene-co-3-benzylthiophene) and polystyrene.[25] For composites consisting of conducting thin cylinders instead of spheres, however, the percolation threshold can be extremely low because the critical volume fraction in this case is determined by the excluded volume per cylinder.[42,43] It has been found, for example, that connected conducting paths exist at conducting polymer volume fractions below 5×10^{-4} in a conducting gel consisting of ultrahigh-molecular-weight polyethylene (in decalin) and P3OT.[40] A percolation threshold of 2.8% therefore suggests a very fine dispersion of the P3OT domains in the semi-IPN, but not completely at the molecular level. The theoretical value of the exponent t, calculated using percolation theory,[37,44] is $t = 1.9 \pm 0.1$. Although the experimentally determined t value of 3.2 is higher, the agreement between the experimental data and theoretical curve is quite satisfactory as seen in Figure 5.

3.5. Optical and Electron Microscopy. All of the data presented thus far confirm the notion that the level of network cross-linking dramatically influences the electrical properties of the P3OT-based semi-IPNs. As might be expected, these variations in properties can be directly related to the different morphological arrangements that develop during network formation. These differences are readily observed in the optical micrographs displayed in Figure 6. The samples imaged in this figure all contain 20% P3OT but different amounts of DVB. Two distinctive phases can be clearly observed in the sample that did not contain any cross-linking agent (Figure 6a). This material is of course not a semi-IPN but rather a simple blend. Since the micrographs are bright-field images, the 10–50-μm bright spheres seen in parts a and

b of Figure 6 are domains of the polystyrene phase. These domains show a faint tint of yellow under the optical microscope, indicating a slight dissolution of the P3OT in the polystyrene phase. The dark regions beyond the bright spheres contain most of the P3OT, but a simple consideration of the fact that the polystyrene phase represents 80% of the blend indicates that polystyrene must also coexist in these regions. The much smaller features in the background of Figure 6a vary upon changing the image focus of the microscope, and they appear to be surface features rather than bulk features. The somewhat blurred rims of the spheres in Figure 6b can be interpreted as the start of mixing of the polystyrene phase and the more continuous P3OT/polystyrene matrix phase.[45] In any event, it is clear that at these cross-linking levels the polystyrene and P3OT phases are highly incompatible and grossly phase separated.

As the cross-linking level increases, the large domains of polystyrene start to break up and become better dispersed throughout the semi-IPN. The 2% DVB sample shown in Figure 6c is a good example of the intermediate stage of this process. With 5% DVB (Figure 6d), the polystyrene domains (bright regions) have been reduced to the order of 3–4 μm. The preferred orientation visible in Figure 6c, where the texture is somewhat oriented from lower left to upper right, most likely is due to the constant flow of the reaction mixture along the flask wall during polymerization. This type of orientation may also exist in other samples prepared by this technique. For example, in Figure 6a, a slight elongation of the polystyrene domains along a preferred direction is discernible. As the amount of DVB increases to 10%, the semi-IPN achieves its highest level of molecular dispersion. The fine structure evident in the 10% DVB sample (Figure 6e) is in fact a surface phenomenon rather than a true representation of the bulk state, indicating an even higher level of molecular mixing of the domains. As will be discussed shortly, this conclusion was confirmed by the STEM results. When the cross-linking amount exceeds 10%, the semi-IPN undergoes an interesting morphological change. The micrograph of the 16% DVB sample presented in Figure 6f displays large dark clusters on the sample surface which are mostly comprised of P3OT. At this higher cross-linking level, syneresis[46] occurs and a large portion of the P3OT is rejected from the cross-linked matrix. In other words, the cross-link density of the polystyrene network has become so high that it is no longer able to support a large amount of finely dispersed P3OT microdomains. A similar phenomenon is also observed in the 23% DVB sample (not shown).

Figure 7 displays the STEM results of the semi-IPN/10% DVB sample. Figure 7a is simply a dark-field TEM micrograph of the sample. The bright areas in the micrograph are sulfur-rich areas, i.e., P3OT-rich phases. Figure 7b is a carbon map of the same sample area displayed in Figure 7a, whereas Figure 7c is a sulfur map of a slightly shifted area. In Figure 7b, the different concentrations of carbon are indicated by different levels of brightness. Because there is only a slight difference between the carbon concentration in polystyrene and that in P3OT, the distribution of carbon seems rather uniform. The dark areas in this graph simply represent thinner sections of the sample. In the sulfur map (Figure 7c), however, segregation of a sulfur-rich phase is clearly visible. The dimensions of these P3OT-rich aggregates are on the order of 1000 Å. Although this value is higher than that found in other semi-IPNs of the second kind (ca. 250 Å),[33,34] it is reasonable when one considers the more rigid nature of the conjugated polymer chains. Figure 7d is a sulfur map on a larger sample area (4.4 × 4.2 μm^2). If there were 1–2-μm P3OT-rich domains in the bulk as suggested by optical microscopy (Figure 7e), it would be possible to identify such features on this scale. The distribution of sulfur, however, appears quite uniform as displayed in Figure 7d, thereby confirming that the features observed in the optical micrograph are surface artifacts. The STEM results therefore show that the 10% DVB sample is best characterized as a semi-IPN with a high level of microdomain dispersion. Thus, the unique properties of this composition can be directly related to its more highly intermixed domain morphology.

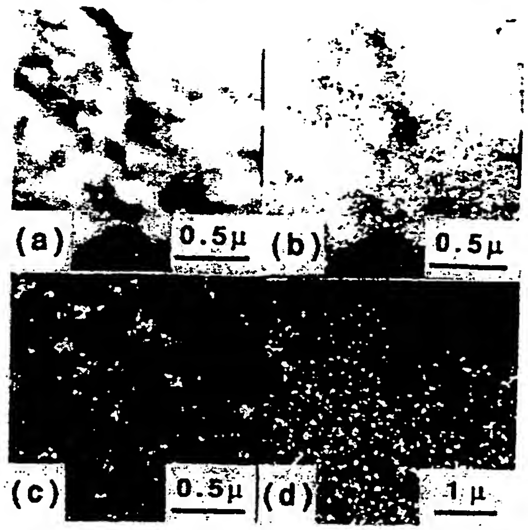

Figure 7. STEM results of the semi-IPN (20% P3OT)/10% DVB: (a) dark-field TEM micrograph of the sample, (b) carbon map of the sample, (c) sulfur map of the sample, (d) sulfur map of the sample (larger area).

4. Conclusions

The results presented in this paper demonstrate that the environmental stability of poly(3-octylthiophene) can be significantly improved by forming semiinterpenetrating networks with cross-linked polystyrene. By controlling the cross-link density of the polystyrene phase, it is possible to use this approach to vary the level of microdomain mixing that occurs in this new multicomponent system. The highest level of microdomain dispersion was achieved in samples prepared with 20% P3OT and 10% of the DVB cross-linking agent. This particular composition produced materials with a high electrical conductivity and an excellent conductivity stability. The improved conductivity stability can be directly traced to the higher level of molecular mixing (at the microdomain scale) that develops in this system during network formation. Our current hypothesis is that this higher level of molecular dispersion of the P3OT phase in the cross-linked polystyrene network restricts the conformational mobility of the P3OT chains, thereby rendering them less susceptible to the thermally induced dedoping process. Another consequence of producing molecularly dispersed, interpenetrating phases is a reduction of the percolation threshold from 16 vol %, which is what is observed in a simple blend, to about 3 vol %. Because the semi-IPN technique involves the manipulation of a soluble con-

ducting polymer in a cross-linkable monomer, this approach can be readily used with a variety of conducting polymers and matrix materials. Thus, this approach provides a new avenue for controlling the mechanical and electrical properties of conjugated polymers.

Acknowledgment. We gratefully acknowledge partial support of this work by AMP Inc., Harrisburg, PA. We also thank Ms. Paula Hammond and Mr. Sam Gido of MIT for their help in preparing the STEM samples.

References and Notes

(1) Wnek, G. E. In Skotheim, T. A., Ed. *Handbook of Conducting Polymers*; Marcel Dekker: New York, 1986; Vol. 1, p 205.
(2) Galvin, M. E.; Wnek, G. E. *Polym. Commun.* 1982, *23*, 795.
(3) Galvin, M. E.; Wnek, G. E. *J. Polym. Sci., Polym. Chem. Ed.* 1983, *21*, 2727.
(4) Rubner, M. F.; Tripathy, S. K.; Georger, J., Jr.; Cholewa, P. *Macromolecules* 1983, *16*, 870.
(5) Niwa, O.; Tamamura, T. *J. Chem. Soc., Chem. Commun.* 1984, 817.
(6) De Paoli, M.-A.; Waltman, R. J.; Diaz, A. F.; Bargon, J. *J. Chem. Soc., Chem. Commun.* 1984, 1015.
(7) Niwa, O.; Hikita, M.; Tamamura, T. *Makromol. Chem., Rapid Commun.* 1985, *6*, 375.
(8) De Paoli, M.-A.; Waltman, R. J.; Diaz, A. F.; Bargon, J. *J. Polym. Sci., Polym. Chem. Ed.* 1985, *23*, 1687.
(9) Niwa, O.; Hikita, M.; Tamamura, T. *Macromolecules* 1987, *20*, 749.
(10) Niwa, O.; Tamamura, T. *Synth. Met.* 1987, *20*, 235.
(11) Lindsey, S. E.; Street, G. B. *Synth. Met.* 1984/85, *10*, 67.
(12) Koga, K.; Iino, T.; Ueta, S.; Takayanagi, M. *Polym. J.* 1989, *21* (4), 303.
(13) Wang, H. L.; Toppare, L.; Fernandez, J. E. *Macromolecules* 1990, *23*, 1053.
(14) Nagasubramanian, G.; DiStefano, S. *J. Electrochem., Soc., Extended Abstr.* 1985, *85-2*, 659.
(15) LaCroix, J.-C.; Diaz, A. F. *Makromol. Chem., Makromol. Symp.* 1987, *8*, 17.
(16) Koga, K.; Yamasaki, S.; Narimatsu, K.; Takayanagi, M. *Polym. J.* 1989, *21* (9), 733.
(17) Rughooputh, S. D. D. V.; Nowak, M.; Hotta, S.; Heeger, A. J.; Wudl, F. *Synth. Met.* 1987, *21*, 41.
(18) Elsenbaumer, R. L.; Jen, K. Y.; Oboodi, R. *Synth. Met.* 1986, *15*, 169.
(19) Österholm, J.-E.; Laakso, J.; Nyholm, P. *Synth. Met.* 1989, *28*, C435.
(20) Nilsson, J.-O.; Gustafsson, G.; Inganäs, O.; Uvdal, K.; Salaneck, W. R.; Österholm, J.-E.; Laakso, J. *Synth. Met.* 1989, *28*, C445.
(21) Isotalo, H.; Stubb, H.; Yli-Lahti, P.; Kuivalainen, P.; Österholm, J.-E.; Laakso, J. *Synth. Met.* 1989, *28*, C461.
(22) Laakso, J.; Österholm, J.-E.; Nyholm, P. *Synth. Met.* 1989, *28*, C467.
(23) Laakso, J.; Österholm, J.-E.; Nyholm, P.; Stubb, H.; Punkka, E. *Synth. Met.* 1990, *37*, 145.
(24) Inganäs, O.; Gustafsson, G. *Synth. Met.* 1990, *37*, 195.
(25) Hotta, S.; Rughooputh, S. D. D. V.; Heeger, A. J. *Synth. Met.* 1987, *22*, 79.
(26) Rueda, D. R.; Cagiao, M. E.; Balatá Callegja, F. J.; Palacios, J. M. *Synth. Met.* 1987, *22*, 53.
(27) Machado, J. M.; Karasz, F. E.; Lenz, R. W. *Polymer* 1988, *29*, 1412.
(28) Schlenoff, J. B.; Machado, J. M.; Glatkowski, P. J.; Karasz, F. E. *J. Polym. Sci., Part B: Polym. Phys.* 1988, *26*, 247.
(29) Machado, J. M.; Schlenoff, J. B.; Karasz, F. E. *Macromolecules* 1989, *22*, 1964.
(30) Machado, J. M.; Karasz, F. E.; Kovar, R. F.; Burnett, J. M.; Druy, M. A. *New Polym. Mater.* 1989, *1* (3), 189.
(31) Machado, J. M.; Masse, M. A.; Karasz, F. E. *Polymer* 1989, *30*, 1992.
(32) Wang, Y.; Rubner, M. F. *Synth. Met.* 1990, *39*, 153.
(33) Sperling, L. H. *Interpenetrating Polymer Networks and Related Materials*; Plenum Press: New York, 1981.
(34) Fitzgerald, J. J.; Landry, C. J. T. *J. Appl. Polym. Sci.* 1990, *40*, 1727.
(35) Tamao, K.; Kodama, S.; Nakajima, I.; Kumada, M. *Tetrahedron* 1982, *38*, 3347.
(36) Sugimoto, R.; Takeda, S.; Gu, H. B.; Yoshino, K. *Chem. Express* 1986, *1* (11), 635.
(37) Zallen, R. *The Physics of Amorphous Solids*; John Wiley & Sons: New York, 1983; Chapter 4.
(38) Fizazi, A.; Moulton, J.; Pakbaz, K.; Rughooputh, S. D. D. V.; Smith, P.; Heeger, A. J. *Phys. Rev. Lett.* 1990, *64* (18), 2180.
(39) Rabeony, M.; Sowa, J. M.; Berluche, E.; Ramakrishnan, S.; Peiffer, D. G. *Dynamics in Small Confining Systems*; Materials Research Society Fall Meeting, Boston, MA, 1990; Materials Research Society: Pittsburgh, PA, 1990.
(40) Scher, H.; Zallen, R. *J. Chem. Phys.* 1970, *53*, 3759.
(41) Powell, M. J. *Phys. Rev. B* 1979, *20* (10), 4194.
(42) Balberg, I.; Anderson, C. H.; Alexander, S.; Wagner, N. *Phys. Rev. B* 1984, *30* (7), 3933.
(43) Suzuki, Y. Y.; Heeger, A. J.; Pincus, P. *Macromolecules* 1990, *23*, 4730.
(44) Zabolitzky, J. G. *Phys. Rev. B.* 1984, *30* (7), 4077.
(45) Sheu, H. R.; El-Aasser, M. S.; Vanderhoff, J. W. *J. Polym. Sci.: Part A: Polym. Chem.* 1990, *28*, 629.
(46) Rempp, P.; Merrill, E. W. *Polymer Synthesis*; Hüthig & Wepf: Basel, Switzerland, 1986; p 246.

Registry No. 3OT, 104934-51-2; (St)(DVB) (copolymer), 9003-70-7; PS, 9003-53-6; $FeCl_3$, 7705-08-0.